

# Quantum effects in thermal conduction: Nonequilibrium quantum discord and entanglement

Lian-Ao Wu<sup>1</sup> and Dvira Segal<sup>2</sup><sup>1</sup>*Department of Theoretical Physics and History of Science, The Basque Country University (EHU/UPV), 48080 Bilbao and IKERBASQUE–Basque Foundation for Science, E-48011, Bilbao, Spain*<sup>2</sup>*Chemical Physics Group, Department of Chemistry and Center for Quantum Information and Quantum Control, University of Toronto, 80 St. George street, Toronto, Ontario, Canada M5S 3H6*

(Received 5 May 2011; published 18 July 2011)

We study the process of heat transfer through an entangled pair of two-level systems, demonstrating the role of quantum correlations in this nonequilibrium process. While quantum correlations generally degrade with increasing the temperature bias, introducing spatial asymmetry leads to an intricate behavior: connecting the qubits unequally to the reservoirs, one finds that quantum correlations persist and *increase* with the temperature bias when the system is more weakly linked to the hot reservoir. In the reversed case, linking the system more strongly to the hot bath, the opposite, more natural behavior is observed, with quantum correlations being strongly suppressed upon increasing the temperature bias.

DOI: 10.1103/PhysRevA.84.012319

PACS number(s): 03.67.Bg, 03.67.Mn, 63.22.-m, 44.10.+i

## I. INTRODUCTION

Understanding thermal energy transfer at the nanoscale has recently become a topic of great interest in nanotechnology [1], with proposals for new devices that can actively control heat conduction and information storage: thermal rectifiers [2], thermal logic operators [3], and memory devices [4]. As some of these devices have already been realized [5,6], one should note that these thermal elements typically have been analyzed within the principles of classical mechanics, operating at room temperature. Assessing the role of quantum effects in the operation of such systems is of fundamental and practical importance, for building quantum devices fighting relaxation and decoherence processes, operating under nonequilibrium conditions.

The typical setup of interest in this context includes a small system, with few degrees of freedom (nanobeam; linear molecule; spin chain), connected at its ends to two large reservoirs (solids; metals), maintained at different temperatures. In the steady-state limit, a constant heat current flows through the system. The thermal conductance of such a nanoscale junction has been primarily simulated using either of the following three approaches: (i) Landauer's formula [7] combined with first-principles calculations of the Hamiltonian force constants [8], (ii) the nonequilibrium Green's function method [9,10], or (iii) classical molecular dynamics simulations [11]. The Boltzmann-Peierls phonon transport theory [12,13], mixed classical-quantum simulations [14], and quantum master equation methods [15–17] are other methods developed for predicting the conductance properties of different objects. For systems with few degrees of freedom, the latter method is of particular interest, as the kinetic equations of motion can be derived, under some approximations, from the fundamental quantum equations of motion, as explained below. For simple model systems, these equations can be analytically solved, providing insight on the microscopic dynamics [16].

Entanglement and quantum discord [18] are quantum correlations with no classical counterpart, which can be used as tools for identifying and distinguishing the quantum aspects in the thermal transport process from the classical ones [19–21]. It

is our objective here to consider a simple (yet involving many-body interactions) thermal conducting junction, to study its transport characteristics within the quantum master equation method, and to evaluate the role of quantum effects in the energy transport process through the entanglement and discord measures. In particular, as the steady-state concurrence in quantum open systems has been already analyzed [19–21], it is of interest to explore its relation to the steady-state discord measure, quantifying nonclassical correlations beyond entanglement.

The particular system examined here includes a pair of a two-level system under a magnetic field, placed in between two thermal reservoirs. We use this model as a case study for illustrating the intricate role of the nonequilibrium condition on quantum correlations in the system. We analytically calculate the amount of entanglement and discord in this model at different bath temperatures, demonstrating that even at relatively high temperatures quantum correlations play a role in the energy transfer process. Furthermore, by introducing asymmetry, we show that, counterintuitively, quantum correlations may be *enhanced* upon increasing the temperature bias across the system, depending on the bias polarity.

## II. MODEL

Our model includes a quantum system coupled to two different thermal reservoirs. The system incorporates two interacting qubits in a magnetic field subjected to the  $XY$  interaction. These qubits, 1 and 2, are separately coupled to independent reservoirs  $H_L$  and  $H_R$ , respectively, maintained in thermal equilibrium at temperatures  $T_\nu$ ,  $\nu = L, R$ . The total Hamiltonian is given by

$$H = H_S + \sum_{\nu} H_{\nu} + V_L + V_R, \quad (1)$$

where the two-qubit Hamiltonian is

$$H_S = \frac{\epsilon}{2}(\sigma_1^z + \sigma_2^z) + \frac{\kappa}{2}(\sigma_1^x \sigma_2^x + \sigma_1^y \sigma_2^y). \quad (2)$$

Here  $\sigma^i$  ( $i = x, y, z$ ) are the Pauli matrices. The system Hamiltonian can be diagonalized to produce the ‘‘system diagonal’’ basis with four states  $n = 1, 2, 3, 4$ ,

$$\begin{aligned} |1\rangle &= \frac{1}{\sqrt{2}}(|\downarrow\uparrow\rangle - |\uparrow\downarrow\rangle), & E_1 &= -\kappa, \\ |2\rangle &= |\downarrow\downarrow\rangle, & E_2 &= -\epsilon, \\ |3\rangle &= |\uparrow\uparrow\rangle, & E_3 &= \epsilon, \\ |4\rangle &= \frac{1}{\sqrt{2}}(|\downarrow\uparrow\rangle + |\uparrow\downarrow\rangle), & E_4 &= \kappa. \end{aligned} \quad (3)$$

The states are ordered assuming that the interspin interaction is strong:  $\kappa > \epsilon > 0$ . As the qubits are identical, the symmetric conditions  $\omega_{43} = \omega_{21}$  and  $\omega_{42} = \omega_{31}$  follow, with  $\omega_{nm} = E_n - E_m$ . We assume that system-bath interactions are separable, and use the following bipartite form:

$$V_v = B_v S^v, \quad (4)$$

with  $B_v$  as a bath operator and  $S^v$  a system operator. Specifically, we use  $S^L = \sigma_1^x$  and  $S^R = \sigma_2^x$ . In the basis of Eq. (3), these operators translate to

$$\begin{aligned} S^L &= \frac{1}{\sqrt{2}}(-|1\rangle\langle 2| + |1\rangle\langle 3| + |2\rangle\langle 4| + |3\rangle\langle 4| + \text{H.c.}), \\ S^R &= \frac{1}{\sqrt{2}}(|1\rangle\langle 2| - |1\rangle\langle 3| + |2\rangle\langle 4| + |3\rangle\langle 4| + \text{H.c.}). \end{aligned} \quad (5)$$

We next calculate the heat current and the quantum entanglement and discord. Note that we have not yet specified a model for the reservoirs, as the calculations can be formally done for different bath realizations [17].

### III. STEADY-STATE DYNAMICS

Under nonequilibrium conditions,  $T_L \neq T_R$ , in the long time limit, we present next the following quantities: (i) the system’s population, (ii) the steady-state heat current, and (iii) the resulting quantum correlations.

#### A. Levels’ population

We follow standard weak coupling schemes [22] and use the Born-Markov approximation. Beginning with the Liouville equation, the method first involves the assumption of weak system-bath interactions. Furthermore, we apply the Markovian limit, assuming that the reservoirs’ characteristic time scales are shorter than the subsystem relaxation time. Under these approximations, a master equation for the state’s population  $P_n$  ( $n = 1, 2, 3, 4$ ) can be readily obtained,

$$\dot{P}_n(t) = \sum_{v,m} |S_{mn}^v|^2 P_m(t) k_{m \rightarrow n}^v - P_n(t) \sum_{v,m} |S_{mn}^v|^2 k_{n \rightarrow m}^v. \quad (6)$$

Details about this derivation (for the two-bath case) are given in Refs. [16] and [17]. Here  $S^v = \sum S_{mn}^v |m\rangle\langle n|$ . The Fermi golden rule transition rates are given by

$$k_{n \rightarrow m}^v = \int_{-\infty}^{\infty} d\tau e^{i\omega_{nm}\tau} \langle B_v(\tau) B_v(0) \rangle_{T_v}, \quad (7)$$

where  $B_v(\tau) = e^{iH_v\tau} B_v e^{-iH_v\tau}$  are interaction picture operators. The thermal average is given by  $\langle O \rangle_{T_v} =$

$\text{Tr}[e^{-H_v/T_v} O] / \text{Tr}[e^{-H_v/T_v}]$ . Note that the rates are evaluated at a specific subsystem frequency. For example, in Eq. (7), the relevant energy scale is  $\omega_{nm} = E_n - E_m$ . Solving Eq. (6) in steady state, we obtain the population

$$\begin{aligned} P_1 &= \frac{W_{12} W_{13}}{(W_{12} + W_{21})(W_{13} + W_{31})}, \\ P_2 &= \frac{W_{21} W_{13}}{(W_{12} + W_{21})(W_{13} + W_{31})}, \\ P_3 &= \frac{W_{12} W_{31}}{(W_{12} + W_{21})(W_{13} + W_{31})}, \\ P_4 &= \frac{W_{21} W_{31}}{(W_{12} + W_{21})(W_{13} + W_{31})}, \end{aligned} \quad (8)$$

where we have introduced the short notation  $W_{mn} = k_{n \rightarrow m}^L + k_{n \rightarrow m}^R$ . Since the qubits are of equal energy and  $|S_{mn}^L|^2 = |S_{mn}^R|^2$ , we have also utilized the fact that  $W_{13} = W_{24}$  and  $W_{34} = W_{12}$  in deriving Eq. (8).

The rate constants depend on the particular choice of the system-bath interaction operator and the bath Hamiltonian. For example, assuming the reservoirs include a collection of harmonic modes and that the bath operator coupled to the system is a displacement operator,

$$H_v = \sum_j \omega_j b_{v,j}^\dagger b_{v,j}, \quad B_v = \sum_j \lambda_{v,j} (b_{v,j}^\dagger + b_{v,j}), \quad (9)$$

the relaxation and excitation rates with  $m > n$  reduce to

$$\begin{aligned} k_{m \rightarrow n}^v &= \Gamma_{B,v}(\omega_{mn}) [n_B^v(\omega_{mn}) + 1], \\ k_{n \rightarrow m}^v &= \Gamma_{B,v}(\omega_{mn}) [n_B^v(\omega_{mn})], \end{aligned} \quad (10)$$

using the definition (7). Here  $\Gamma_{B,v}(\omega) = 2\pi \sum_j \lambda_{v,j}^2 \delta(\omega - \omega_j)$  and  $n_B^v(\omega) = [e^{\omega/T_v} - 1]^{-1}$  is the Bose-Einstein distribution. Another physical setup is the spin reservoir, including a collection of  $P$  noninteracting spins,

$$H_v = \sum_{p=1}^P h_{v,p}, \quad B_v = \sum_{p=1}^P b_{v,p}. \quad (11)$$

$h_{v,p}$  and  $b_{v,p}$  are single-spin operators. Each spin is described by the two eigenstates ( $i = 0, 1$ )  $|i\rangle_p$  and eigenenergies  $\epsilon_p(i)$ . In this case, the relaxation rate becomes

$$k_{m \rightarrow n}^v = \Gamma_{S,v}(\omega_{mn}) n_S^v(-\omega_{mn}), \quad (12)$$

with the spin occupation factor  $n_S^v(\omega) = [e^{\omega/T_v} + 1]^{-1}$  and the effective spin-bath-system coupling  $\Gamma_{S,v}(\omega) = 2\pi \sum_p |\langle 0|_p b_{v,p} |1\rangle_p|^2 \delta(\omega + \epsilon_p(0) - \epsilon_p(1))$ . For details, see Ref. [17].

#### B. Heat current

Formally, the expectation value of the current, calculated, e.g., at the left contact, is given by  $J_L = \frac{i}{2} \text{Tr}([H_L - H_S, V_L] \rho_T)$ , where  $\rho_T$  is the total density matrix [23]. In steady state, the expectation value of the interaction is zero,  $\text{Tr}(\frac{\partial V_L}{\partial t} \rho_T) = i \text{Tr}([H_L + H_S, V_L] \rho_T)$ , and this expression reduces to  $J_L = i \text{Tr}([V_L, H_S] \rho_T)$ . Using the system-diagonal representation, it is straightforward to show that the steady-state current becomes [17]

$$J_L = i \sum_{m,n} \omega_{mn} S_{mn}^L \text{Tr}_B [B_L(\rho_T)_{mn}], \quad (13)$$

where  $\omega_{mn} = E_m - E_n$ . Under the Born-Markov approximation used above to resolve the population dynamics, a second-order expression for the steady-state current can be further obtained [17]:

$$J_L = \frac{1}{2} \sum \omega_{mn} |S_{mn}^L|^2 P_n (k_{n \rightarrow m}^L - k_{n \rightarrow m}^R). \quad (14)$$

We apply this expression on the two-qubit model. A somewhat tedious calculation shows that the current is given by a sum of two terms,

$$J_L = \frac{\omega_{21} (k_{1 \rightarrow 2}^L k_{2 \rightarrow 1}^R - k_{2 \rightarrow 1}^L k_{1 \rightarrow 2}^R)}{2 [k_{1 \rightarrow 2}^L + k_{2 \rightarrow 1}^R + k_{2 \rightarrow 1}^L + k_{1 \rightarrow 2}^R]} + \frac{\omega_{31} (k_{1 \rightarrow 3}^L k_{3 \rightarrow 1}^R - k_{3 \rightarrow 1}^L k_{1 \rightarrow 3}^R)}{2 [k_{1 \rightarrow 3}^L + k_{3 \rightarrow 1}^R + k_{3 \rightarrow 1}^L + k_{1 \rightarrow 3}^R]}. \quad (15)$$

### C. Concurrence

The entanglement of formation is a monotonically increasing function of Wootters' concurrence [24]. We calculate next the nonequilibrium concurrence in the two-qubit model. The states  $|1\rangle$  and  $|4\rangle$  are entangled, and the nature of the entanglement may remain in the final steady state, which is described by the diagonal reduced density matrix  $\rho_d = \text{diag}(P_1, P_2, P_3, P_4)$ , in the eigenbasis of the system Hamiltonian  $H_S$ . On the other hand, in the uncoupled basis  $|\downarrow\downarrow\rangle, |\downarrow\uparrow\rangle, |\uparrow\downarrow\rangle, |\uparrow\uparrow\rangle$ , the reduced density matrix is given by a nondiagonal form,

$$\rho = \begin{pmatrix} P_2 & 0 & 0 & 0 \\ 0 & \frac{P_1+P_4}{2} & \frac{P_4-P_1}{2} & 0 \\ 0 & \frac{P_4-P_1}{2} & \frac{P_1+P_4}{2} & 0 \\ 0 & 0 & 0 & P_3 \end{pmatrix}. \quad (16)$$

Using the general form given in, e.g., [25], the concurrence can be expressed in the uncoupled basis by

$$C(T_L, T_R) = \max(2P_{\max} - P_1 - P_4 - 2\sqrt{P_2 P_3}, 0), \quad (17)$$

where  $P_{\max} = \max(P_1, P_4, \sqrt{P_2 P_3})$ . This function in general depends on the temperatures of both thermal baths.

### D. Discord

Quantum discord [18], quantifying nonlocal correlations, is given by the difference between the quantum mutual information  $\mathcal{I}(\rho)$  and the classical correlation  $\mathcal{C}(\rho)$ ,

$$\mathcal{Q}(\rho) = \mathcal{I}(\rho) - \mathcal{C}(\rho). \quad (18)$$

The analytical expressions for the classical correlation and the quantum discord were obtained for a class of  $X$  states in Ref. [25]. Adjusting these expressions to our model, the quantum mutual information can be written in terms of the steady-state populations (8) as

$$\mathcal{I}(\rho) = 2 - \log_2[(1 - P_2 + P_3)^{1-P_2+P_3} (1 + P_2 - P_3)^{1+P_2-P_3}] + P_1 \log_2 P_1 + P_2 \log_2 P_2 + P_3 \log_2 P_3 + P_4 \log_2 P_4, \quad (19)$$

whereas the classical correlation is given by

$$\mathcal{C}(\rho) = 1 - \frac{1}{2} \log_2[(1 - P_2 + P_3)^{1-P_2+P_3} \times (1 + P_2 - P_3)^{1+P_2-P_3}] - \min\{S_1, S_2\}. \quad (20)$$

Here

$$S_1 = -P_2 \log_2 \left( \frac{2P_2}{1 + P_2 - P_3} \right) - \left( \frac{P_1 + P_4}{2} \right) \log_2 \left( \frac{P_1 + P_4}{1 + P_2 - P_3} \right) - \left( \frac{P_1 + P_4}{2} \right) \log_2 \left( \frac{P_1 + P_4}{1 - P_2 + P_3} \right) - P_3 \log_2 \left( \frac{2P_3}{1 - P_2 + P_3} \right) \quad (21)$$

and

$$S_2 = 1 - \frac{1}{2} \log_2[(1 - K)^{1-K} (1 + K)^{1+K}]. \quad (22)$$

The coefficient  $K$  is defined as  $K = \sqrt{(P_2 - P_3)^2 + (P_1 - P_4)^2}$ .

## IV. EXAMPLES

In what follows, we analyze the quantum correlations, concurrence, and discord, for various nonequilibrium conditions, showing that quantum discord survives at relatively high temperatures where concurrence is zero. We also study an asymmetric scenario demonstrating that quantum correlations may exist even at large temperature biases. We will typically use the following parameters: spin energy  $\epsilon = 0.2$  and large spin-spin interaction  $\kappa = 1$ . We will also assume that the relaxation rates do not depend on energy, and thus treat them as constants,  $\Gamma_{B,v}$  and  $\Gamma_{S,v}$ . The factor  $1/\sqrt{2}$  in Eq. (5) is absorbed into the definition of the rates  $\Gamma$ .

We begin our analysis with an equilibrium situation,  $T_a = T_L = T_R$ , and compare the concurrence and the discord measures at different temperatures. Figure 1 shows that at very low temperatures both measures yield the same result. At higher temperatures (yet  $T_a < \kappa$ ), concurrence is slightly larger than discord. At even higher temperatures,  $T_a > \kappa$ , concurrence suddenly diminishes [26], while quantum discord is still finite, slowly decreasing to zero. This is in accord with the fact that discord quantifies nonclassical correlations beyond entanglement. Generally, both quantum correlations decay with temperature due to thermal relaxation effects. As can be inferred from the inset, when the ground-state population falls below  $\sim 1/2$ , the concurrence dies. We also found that these observations were not sensitive to the reservoir's properties, and similar trends were obtained using either boson or spin baths.

Figure 2 displays the nonequilibrium thermal correlations, keeping  $T_L$  fixed and changing  $T_R$ . In the classical limit, at high temperatures (top panel) the discord overcomes the concurrence, even when  $T_R$  is low. In contrast, at low temperatures (bottom panel), the opposite trend is observed until a crossover value beyond which the concurrence dies [26], yet the discord is finite. While in Fig. 2 bosonic reservoirs have been adopted, Fig. 3 displays the nonequilibrium thermal

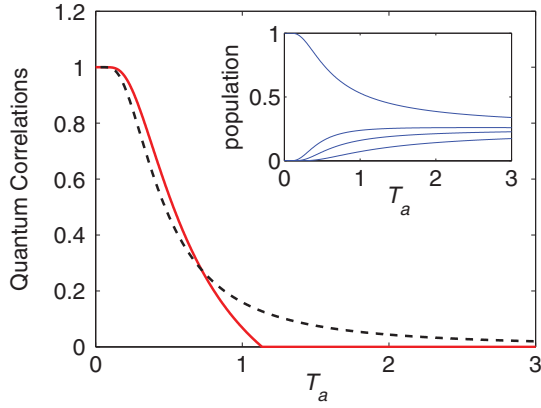


FIG. 1. (Color online) Concurrence (full) and discord (dashed) in an equilibrium system,  $T_a = T_L = T_R$ . The inset displays the levels population, top ( $P_1$ ) to bottom ( $P_4$ ). The physical parameters are  $\epsilon = 0.2$  and  $\kappa = 1$ . Bosonic reservoirs were adopted.

correlations using spin baths. The main difference noted is that when  $T_L$  is quite high and  $T_R$  is low [see Fig. 3(a)], the spin-bath case shows that concurrence is higher than discord, while the opposite behavior is observed in Fig. 2(a). This observation is in accord with the notion that spin reservoirs are “more quantum” than harmonic baths in the sense that harmonic modes can be represented by two-level systems (spins) at low enough temperatures.

Next, we explore the role of spatial asymmetry on the survival of quantum correlations in (temperature) driven systems. Thermal rectification, an asymmetry of the heat current for forward and reversed temperature gradients, has been extensively analyzed in the past decade [2,5,17]. In a desirable rectifier, the system behaves as an excellent heat conductor in one direction of the temperature bias, while for the opposite direction it effectively acts as an insulator. It is agreed that junctions incorporating anharmonic interactions with some sort of spatial asymmetry should demonstrate this effect. The two-qubit model, prepared with some asymmetry,

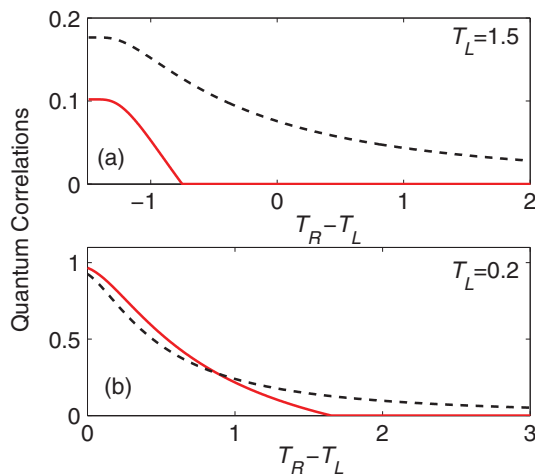


FIG. 2. (Color online) (a) Nonequilibrium thermal correlations for a pair of qubits coupled to boson baths. Concurrence (full) and discord (dashed) for  $T_L = 1.5$ ,  $T_R$  is modified. (b) Same for  $T_L = 0.2$ . The two-qubit parameters are  $\epsilon = 0.2$  and  $\kappa = 1$  and we set  $\Gamma_{B,v} = 1$ .

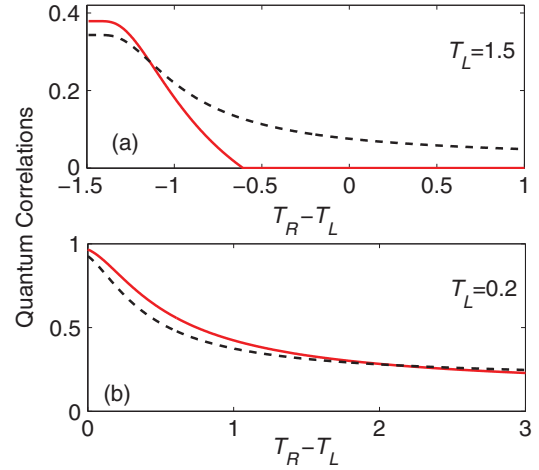


FIG. 3. (Color online) (a) Nonequilibrium thermal correlations for a pair of qubits coupled to spin baths. Concurrence (full) and discord (dashed) for  $T_L = 1.5$ ,  $T_R$  is modified. (b) Same for  $T_L = 0.2$ . The two-qubit parameters are  $\epsilon = 1$  and  $\kappa = 0.2$ , and we set  $\Gamma_{S,v} = 1$ .

e.g., assuming that the qubits asymmetrically couple to, e.g., bosonic reservoirs,  $\Gamma_{B,L} \neq \Gamma_{B,R}$ , is expected to behave as a thermal rectifier.

Figure 4 indeed shows the emergence of the thermal rectifying effect upon turning on the asymmetry. The current in Fig. 4(b) is symmetric, since  $\Gamma_{B,L} = \Gamma_{B,R}$ . In contrast, in Fig. 4(d) the heat current is larger (in magnitude) when the system is more strongly linked to the cold reservoir ( $T_L < T_R$  and  $\Gamma_{B,L} > \Gamma_{B,R}$ ) [2]. Here the averaged temperature is  $T_a = 1$  with  $T_L = T_a + \Delta T$  and  $T_R = T_a - \Delta T$ . While the effect of thermal rectification is well understood, here we demonstrate that the transition between the fairly conducting phase

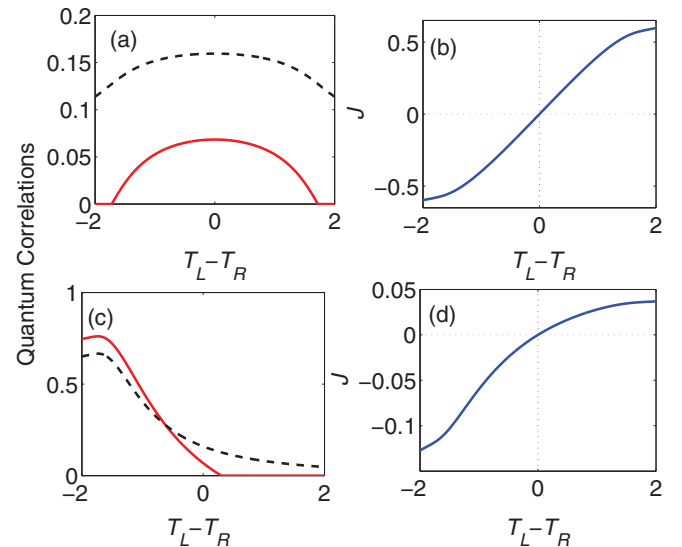


FIG. 4. (Color online) Concurrence (full) and discord (dashed) in symmetric (a) and asymmetric systems (c);  $T_a = 1$  is fixed and the temperatures at the two ends are modulated,  $T_L = T_a + \Delta T$ ,  $T_R = T_a - \Delta T$ . In the symmetric case,  $\Gamma_{B,L} = \Gamma_{B,R} = 1$ . Asymmetry is introduced by taking  $\Gamma_{B,L}/\Gamma_{B,R} = 20$  with  $\Gamma_{B,L} = 1$ . Panels (b) and (d) further display the current for the symmetric and asymmetric cases, respectively. In all panels,  $\epsilon = 0.2$  and  $\kappa = 1$ .

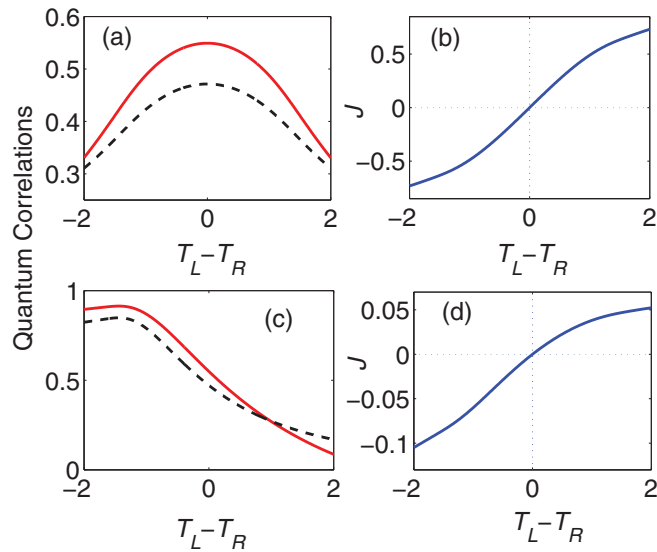


FIG. 5. (Color online) Concurrence (full) and discord (dashed) in symmetric (a) and asymmetric systems (c). Panels (b) and (d) display the current for the symmetric and asymmetric situations, respectively. Parameters are the same as in Fig. 4, but the interspin interaction has been increased to  $\kappa = 2$ .

( $\Delta T < 0$ ) and the poorly conducting phase ( $\Delta T > 0$ ) corresponds to a turnover in the transport mechanism. In the symmetric setup, discord and concurrence are symmetric functions [see Fig. 4(a)]:  $C(\Delta T) = C(-\Delta T)$  and  $Q(\Delta T) = Q(-\Delta T)$ . Figure 4(c) shows a different behavior in the presence of asymmetry: when the bias is negative, quantum correlations persist; however, for the opposite polarity, the concurrence is zero and discord is diminishing.

We can reason this behavior by noting that when the system is more strongly attached to the cold bath,  $\Gamma_{B,L} > \Gamma_{B,R}$  and  $T_R > T_L$ , the ground-state population is larger than that expected in the opposite case. Since the ground state is an entangled (singlet) state,  $|1\rangle = \frac{1}{\sqrt{2}}(|\downarrow\uparrow\rangle - |\uparrow\downarrow\rangle)$ , its large population reflects an energy transmission process assisted by a quantum correlated system state.

By further increasing  $\kappa$ , one can extend the range over which quantum correlations survive; see Fig. 5. For the asymmetric setup, again we note that when  $T_L < T_R$  the current is large, in comparison to the opposite polarity, and that entanglement measures are close to unity. For the reversed

case,  $T_L > T_R$ , the current magnitude is lowered, and quantum correlations are being suppressed. In particular, for  $T_L - T_R = -2$ , discord is large,  $Q \sim 1$ , while at  $T_L - T_R = 2$  it is reduced by an order of magnitude,  $Q \sim 0.1$ . Another interesting observation is that both discord and concurrence display a nonmonotonic behavior at large negative bias, reflected in a small maxima around  $\Delta T \sim -1.7$  [19–21].

To conclude this section, by switching the sign of the temperature bias, one can control the magnitude of the heat current in asymmetric spin chains and the underlying transport mechanism, as reflected by the survival or suppression of quantum correlations in the system.

## V. SUMMARY

We detailed here a simple model of a many-body open quantum system that could be analytically solved, useful for analyzing the role of the temperature gradient on quantum correlations in a conducting nanojunction. Our calculations manifest that, for symmetric systems under large temperature gradients and at high temperatures, quantum discord can be maintained, slowly decaying with  $\Delta T$ , whereas concurrence typically dies. In the presence of asymmetry, we found that quantum correlations can survive in one direction of the temperature gradient, while they diminish when reversing the bias direction.

The present analysis could be generalized for describing transport and quantum correlations in longer-linear spin chains. One could also treat other systems, e.g., large spins, or adopt unequal reservoirs at the two ends, for example, assuming the system is coupled to both a solid and a metal [17]. By complementing transport studies with the calculation of quantum correlations, one can estimate and corroborate the role of quantum effects in the transport process. This might be useful for building quantum devices operating in noisy-thermal environments under nonequilibrium conditions [27].

## ACKNOWLEDGMENTS

L.-A.W. has been supported by the Ikerbasque Foundation Start-up, the CQIQC grant, the Basque Government (grant IT472-10) and the Spanish MEC (Project No. FIS2009-12773-C02-02). D.S. acknowledges support from the NSERC discovery grant.

[1] Y. Dubi and M. Di Ventra, *Rev. Mod. Phys.* **83**, 131 (2011).  
 [2] M. Terraneo, M. Peyrard, and G. Casati, *Phys. Rev. Lett.* **88**, 094302 (2002); D. Vainchtein and I. Mezić, *ibid.* **93**, 84301 (2004); D. Segal and A. Nitzan, *ibid.* **94**, 034301 (2005); B. Hu, L. Yang, and Y. Zhang, *ibid.* **97**, 124302 (2006); L. A. Wu and D. Segal, *ibid.* **102**, 095503 (2009).  
 [3] L. Wang and B. Li, *Phys. Rev. Lett.* **99**, 177208 (2007).  
 [4] L. Wang and B. Li, *Phys. Rev. Lett.* **101**, 267203 (2008).  
 [5] C. W. Chang, D. Okawa, A. Majumdar, and A. Zettl, *Science* **314**, 1121 (2006).

[6] R. Xie *et al.*, *Adv. Funct. Mater.* **21**, 1602 (2011).  
 [7] L. G. C. Rego and G. Kirczenow, *Phys. Rev. Lett.* **81**, 232 (1998).  
 [8] I. Savic, N. Mingo, and D. A. Stewart, *Phys. Rev. Lett.* **101**, 165502 (2008); D. A. Stewart, I. Savic, and N. Mingo, *Nano Lett.* **9**, 81 (2008).  
 [9] N. Mingo and L. Yang, *Phys. Rev. B* **68**, 245406 (2003); N. Mingo, *ibid.* **74**, 125402 (2006).  
 [10] J.-S. Wang, J. Wang, and J. T. Lü, *Eur. Phys. J. B* **62**, 381 (2008).  
 [11] S. Lepri, R. Livi, and A. Politi, *Phys. Rep.* **377**, 1 (2003); A. Dhar, *Adv. Phys.* **57**, 457 (2008).

- [12] P. Carruthers, *Rev. Mod. Phys.* **33**, 92 (1961).
- [13] H. Spohn, *J. Stat. Phys.* **124**, 1041 (2006).
- [14] J.-S. Wang, *Phys. Rev. Lett.* **99**, 160601 (2007).
- [15] H. Wichterich, M. J. Henrich, H. P. Breuer, J. Gemmer, and M. Michel, *Phys. Rev. E* **76**, 031115 (2007); Y. Yan, C. Q. Wu, G. Casati, T. Prosen, and B. Li, *Phys. Rev. B* **77**, 172411 (2008);
- [16] D. Segal, *Phys. Rev. B* **72**, 165426 (2005).
- [17] L.-A. Wu, C. X. Yu, and D. Segal, *Phys. Rev. E* **80**, 041103 (2009).
- [18] H. Ollivier and W. H. Zurek, *Phys. Rev. Lett.* **88**, 017901 (2001); W. H. Zurek, *Rev. Mod. Phys.* **75**, 715 (2003).
- [19] L. Quiroga, F. J. Rodriguez, M. E. Ramirez, and R. Paris, *Phys. Rev. A* **75**, 032308 (2007).
- [20] I. Sinaysky, F. Petruccione, and D. Burgarth, *Phys. Rev. A* **78**, 062301 (2008).
- [21] X. L. Huang, J. L. Guo, and X. X. Yi, *Phys. Rev. A* **80**, 054301 (2009).
- [22] H. P. Breuer and F. Petrucci, *The Theory of Open Quantum Systems* (Oxford University Press, New York, 2002).
- [23] L.-A. Wu and D. Segal, *J. Phys. A* **42**, 025302 (2009).
- [24] W. K. Wootters, *Phys. Rev. Lett.* **80**, 2245 (1998).
- [25] B. Li, Z.-X. Wang, and S.-M. Fei, *Phys. Rev. A* **83**, 022321 (2011).
- [26] J. H. Eberly and T. Yu, *Science* **316**, 555 (2007); M. P. Almeida *et al.*, *ibid.* **316**, 579 (2007).
- [27] Y. Yan, C.-Q. Wu, and B. Li, *Phys. Rev. B* **79**, 014207 (2009).